Testing and characterization of high-temperature degradation performance of para-aramid fibres

DOI: 10.35530/IT.075.01.2023115

CHUNYAN ZHU
YANPING LIN
XIANGAI ZHANG
CHEN YANG

ABSTRACT – REZUMAT

Testing and characterization of high-temperature degradation performance of para-aramid fibres

Para-aramid fibres possess excellent properties, including high modulus, high strength, and high-temperature resistance, making them highly practical and cost-effective reinforcement materials. To further analyse the usage performance of para-aramid fibres under extreme conditions and explore their degradation behaviour and mechanisms at high temperatures, this paper investigates para-aramid fibres through high-temperature annealing. Various tests, including thermogravimetric analysis, infrared spectroscopy, X-ray diffraction, Ubbelohde viscometry, and universal material testing, were employed to analyse changes in the thermal degradation temperature, molecular structure, and mechanical properties of para-aramid fibres. Tests have shown that after high-temperature treatment of para-aramid fibres, different protruding particles and pits appear on the surface of the fibres, and the molecular structure gradually undergoes cleavage and cross-linking. This results in varying degrees of increase in the crystallinity, intrinsic viscosity, and apparent grain size of crystal planes in different directions of the para-aramid fibres with rising temperatures. On the other hand, the degree of orientation, the rate of the second type of lattice distortion, thermal performance, and mechanical properties show a declining trend. The thermal degradation conforms to the kinetics of a second-order reaction.

Keywords: *microscopic morphology, viscosity, activation energy, mechanical properties, mechanism, molecular structure, para-aramid, thermal degradation*

Testarea și caracterizarea performanței de degradare la temperatură înaltă a fibrelor para-aramidice

Fibrele para-aramidice posedă proprietăți excelente, inclusiv modul înalt, rezistență ridicată și rezistență la temperatură ridicată, făcându-le materiale de armare extrem de practice și rentabile. Pentru a analiza în continuare performanța de utilizare a fibrelor para-aramidice în condiții extreme și pentru a explora comportamentul și mecanismele de degradare ale acestora la temperaturi ridicate, această lucrare investighează fibrele para-aramidice prin tratament la temperatură înaltă. Diverse teste, inclusiv analiza termogravimetrică, spectroscopie în infraroșu, difracția de raze X, vâscozimetria Ubbelohde și testarea universală a materialelor, au fost utilizate pentru a analiza modificările temperaturii de degradare termică, structurii moleculare și proprietăților mecanice ale fibrelor para-aramidice. Testele au arătat că, după tratamentul la temperatură înaltă a fibrelor para-aramidice, pe suprafața fibrelor apar diferite particule proeminente și orificii, iar structura moleculară suferă treptat scindare și reticulare. Acest lucru are ca rezultat grade diferite de creștere a cristalinității, a vâscozității intrinseci și a mărimii aparente a granulelor planurilor cristalografice în diferite direcții ale fibrelor para-aramidice odată cu creșterea temperaturii. Pe de altă parte, gradul de orientare, rata celui de-al doilea tip de distorsiune a rețelei, performanța termică și proprietățile mecanice arată o tendință de scădere. Degradarea termică se conformează cineticii unei reacții de ordinul doi.

Cuvinte-cheie: *morfologie microscopică, viscozitate, energie de activare, proprietăți mecanice, mecanism, structura moleculară, para-aramidic, degradare termică*

INTRODUCTION

This experimental study focuses on para-aramid fibres produced by Shengma Corporation in Pingdingshan, China. The research investigates the molecular structure, thermal, and mechanical property changes of these fibres after baking at temperatures of 20°C, 200°C, 350°C, and 500°C for 50 minutes. The study aims to analyse the influence of high-temperature treatment on the physicochemical degradation performance of para-aramid fibres and explore the high-temperature degradation mechanisms of these fibres. As widely recognized, the chemical name of para-aramid fibre is “Poly-p-phenylene terephthalamide”, abbreviated as PPTA. Its chemical structure consists of para-linked benzene amide units, with the benzene rings and amide bonds forming an π-conjugated structure. The macromolecular configuration is characterized by an axially extended chain, a cross-linked network, and a high degree of internal rotation. The regular molecular arrangement, along with high crystallinity and orientation, imparts para-aramid fibres with high strength, high modulus, acid and alkali resistance, and high-temperature resistance [1–3]. These fibres find extensive applications in advanced fields such as

industrial reinforcement, papermaking, aerospace, and defence industries [4–6].

In recent years, with the expansion of para-aramid fibre applications and their increased use across various industries, research on the performance of para-aramid fibres has become increasingly profound. Given that para-aramid fibres are predominantly used in high-temperature environments, studying their thermal degradation behaviour has become imperative. In 1977, Brown et al. used DTA, TG, and TMA techniques to evaluate the high-temperature resistance of Kevlar® fibres. Tests showed that the degree of oxidation reaction in Kevlar® fibres was more severe than their high-temperature resistance [7]. In 1982, Brown and Power used pyrolysis/gas chromatography-mass spectrometry to test the thermal degradation of Kevlar® fibres in the 300–700°C range analysed the degradation products at each temperature range and explained the thermal degradation mechanism [8, 9]. In the same year, Power studied the thermal degradation of aromatic polyamide Kevlar® fibres in air and vacuum using electron spin resonance spectroscopy. The results showed that the presence of oxygen reduced the stability of Kevlar® fibres, causing the aromatic NH and amide NH-CO bonds in Kevlar® fibres to break in the initial stage of thermal degradation. Subsequent stages of thermal degradation confirmed that the participation of oxygen led to an increase in the free radical g-factor, with oxygen acting as a substituent functional group, integrating into the aromatic polyamide, and leading to the detachment of oxygen-containing structural units in the course of homolytic reactions, thus completing thermo-oxidative degradation [10]. In 1982, YP Khanna and others tested the thermal stability, thermal form stability, and thermal transition properties of substituted and unsubstituted aromatic polyamides. The results showed that the exothermic temperature range of polyamides was concentrated between 630–700°C, and although substituents reduced the thermal stability of Kevlar® fibres, they improved their thermo-oxidative stability [11]. In 1984, Wu tested the solubility, intrinsic viscosity, modulus, and strength of para-aramid fibres after heat treatment, concluding that the degradation of para-aramid fibres was due to branching and crosslinking between molecules in the fibres [12]. In 1989, Hindeleh et al. studied the effect of thermal ageing and degradation on the microstructure of Kevlar® fibres. Tests showed that the crystallinity of Kevlar® fibres decreased with temperature, being 75.5% at 350°C and 51% at 500°C. The microcrystalline size remained constant before 250°C and then decreased. TGA tests showed that mass loss intensified with increasing dimensions, with about 1% loss at 350°C, 3.9% at 450°C, and 20.4% at 657°C [13].

In 1994, Zhang tested the physicochemical property changes of para-aramid fibres during pyrolysis. The fibres were heated to 300–710 °C in flowing nitrogen and static air and maintained for 10–30 seconds.

Tests showed that the skin-core structure, mechanical properties, and degree of crystal structure damage in para-aramid fibres all intensified with increasing temperature, and the damage to para-aramid fibres in high-temperature oxygen was greater than in a nitrogen atmosphere [14]. In 2000, Yue et al. analysed the effect of 2–8 hours of heat treatment at 100–300°C on the mechanical properties of Kevlar® yarns. Tests showed that the tensile stress and strength of Kevlar® yarns decreased with increasing temperature, while research by Iyer et al. indicated that the duration of heating at a constant temperature had little effect on the tensile strain and strength of para-aramid fibres [15, 16]. In 2004, James et al. used TG and SCS techniques to test the compressive properties of heat-treated Kevlar® fibres, characterizing the relationship between hydrogen bond breakage, crosslinking, and fibre compressibility, and used Fourier-transform infrared spectroscopy to describe the crosslinking of the cortex and hydrogen bond breakage in the core of para-aramid fibres at 400°C, 440°C, and 470°C [17]. In 2008, Xinwei et al. used TGA-DTA/MS to test the thermal degradation of para-aramid fibres under different atmospheric conditions. The results showed that the thermal degradation of para-aramid fibres in argon was endothermic, while in air it was exothermic [18]. In 2010, Renqin et al. tested the thermal degradation of Kevlar® fibres in an inert atmosphere and at different heating rates, concluding that the activation energy of thermal decomposition of Kevlar® fibres was 210.93 KJ/mol, and the reaction order of thermal decomposition kinetics was first-order [19]. In 2014, Fang-Long et al. conducted thermogravimetric analysis and differential thermal analysis of polysulfone aramid fibres in nitrogen and air atmospheres, showing that at a heating rate of 10 K/min, the initial degradation temperature was 375°C in nitrogen and 410°C in air. When the temperature reached 800°C, the fibres lost all their mass in the air. The differential thermogravimetric curve showed two distinct exothermic peaks, leading to the conclusion that the degradation of polysulfone aramid occurred in a two-step process [20]. In 2019, Naveen et al. used hand lay-up and hot-pressing methods to make composites of different ratios using Kevlar 29 (K) and Cocos nucifera sheath (CNS) as materials. Tests showed that when the ratio of Kevlar 29 (K) and Cocos nucifera sheath (CNS) was 75/25, the composite had better rigidity, thermal stability, and renewability [21]. However, current research on heat treatment of para-aramid fibres is extensive, but the process of changes in the surface functional groups of para-aramid fibres after heat treatment is not clear, and the specific process of increased oxygen content on the fibre surface after heat treatment is also not clear. Therefore, investigating the thermal oxidation behaviour of para-aramid fibres, characterizing changes in their surface groups during heat treatment, and understanding the conditions of thermal oxidation treatment are of paramount importance.

Through this study, we can further delve into the impact of molecular structural changes in para-aramid fibres under different temperature conditions

on their thermal and mechanical properties. This research provides valuable insights into the high-temperature degradation mechanisms of para-aramid fibres and offers a reference for their further development and utilization.

EXPERIMENTAL SECTION

Materials and instruments

Materials: Para-aramid fibres (linear density: 70 tex/187f), supplied by Shennong Company, Pingdingshan, China; Potassium bromide (analytical grade), purchased from Hongyan Chemical Reagent Factory, Tianjin, China.

Instruments: SU3500 Scanning Electron Microscope (Hitachi High-Tech, Shanghai, China); Universal Material Testing Machine (INSTRON 5590), manufactured by Instron Corporation, USA; Thermogravimetric Analyzer (TG/DTG-DSC, TG209F3), supplied by NETZSCH Scientific Instruments Trading (Shanghai) Co., Ltd.; Electronic Analytical Balance (FA3004), provided by Shanghai Yanfeng Electronic Technology Co., Ltd.; Constant Temperature and Humidity Test Chamber (KSD-TH-80L), manufactured by Dongguan Keiside Testing Instrument Co., Ltd.; Tabletop Forced Air Drying Oven (DHG-9035A), manufactured by Wuhan Lihui Environmental Detection Equipment Co., Ltd.; High-Temperature Muffle Furnace (YB-1700A), supplied by Luoyang Bolaimante Test Electric Furnace Co., Ltd.; Ubbelohde Viscometer (1833), manufactured by Qianbo Teaching Instruments Co., Ltd., Tianchang, China; Fourier Transform Infrared Spectrometer (FT-IR, Nicolet iS10), distributed by YuNuo Industry (Shanghai) Co., Ltd.; X-ray Diffractometer (XRD, XRD-7000S), provided by Shimadzu (China) Management Co., Ltd.

Sample preparation

Sample treatment

Para-aramid fibre samples were placed in a muffle furnace and heated for 50 minutes at temperatures of 20°C, 200°C, 350°C, and 500°C.

Performance testing and characterization

Characteristic viscosity testing

A certain amount of para-aramid fibre, both before and after high-temperature treatment, was placed in a forced air drying oven at 110°C for 5 hours. After removal, it was dissolved in a concentrated sulfuric acid solution with a mass fraction of 98%, resulting in a concentration of 0.05 g/dl for para-aramid sulfuric acid solution. The relative viscosity of the dissolved sulfuric acid solution was measured using a Ubbelohde viscometer, and the characteristic viscosity of para-aramid fibres before and after high-temperature treatment was calculated following reference [3].

FT-IR Testing

Para-aramid fibres, both before and after high-temperature treatment, were crushed into powder and then mixed with potassium bromide before being pressed into sample pellets. The FT-IR spectra were recorded at a resolution of 4 cm^{-1} in the range of 4000 to 400 cm^{-1}, with 36 scans per sample. FT-IR testing was conducted to analyse the structure of para-aramid fibres.

Crystalline structural property testing

XRD testing was performed to investigate the crystalline structural properties of para-aramid fibre samples. Using Cu target, Kα radiation with a wavelength of 0.1541 nm, voltage of 40 kV, and current of 40 mA, diffraction scans of the meridian and equatorial lines of para-aramid samples were conducted in transmission mode. The orientation diffraction scan was carried out at 2θ = 22.8° corresponding to the 200 crystal plane of para-aramid samples, with a scanning angle range from 5 to 45 degrees. The measured diffraction curve parameters were corrected for factors such as absorption, angle factors, polarization, and scattering, following reference [22], and used for the calculation of crystalline structural parameters. Data obtained from the tests were subjected to peak fitting using the Gauss+Lor Area function and analysed based on equation 1 following reference [23] to calculate the crystallinity of para-aramid fibre samples.

$$X_d = \left[1 - \frac{S_a}{S_a + S_{cr}}\right] \times 100\% \quad (1)$$

In the equations below, X_d represents the crystallinity of para-aramid fibre samples. S_a denotes the area of the amorphous diffraction peak (corresponding to 2θ = 21°) in para-aramid fibre samples. S_{cr} refers to the area of the crystalline diffraction peaks (corresponding to the peaks at 110, 200, and 002) in para-aramid fibre samples.

For the meridional (002) diffraction scan of para-aramid fibre samples, Gaussian functions were selected for peak fitting. The apparent grain size of para-aramid fibre samples was calculated according to Scherer's formula (equation 2) [24].

Simultaneously, peak fitting was performed for the diffraction peaks at 002, 004, and 006 crystallographic planes, and based on equations 2 and 3 references, the second-class lattice distortion parameters for para-aramid fibre samples were calculated.

$$L = \frac{k\lambda}{\beta \cos\theta} \quad (2)$$

$$G = \sqrt{\frac{d}{360\lambda}} \times \sqrt{\frac{\Delta(\beta\cos\theta)}{\Delta h^2}} \quad (3)$$

In the equations below, L is the apparent grain size of para-aramid fibre samples, θ – the Bragg angle (°), β – the half-width of the diffraction peak (calculated in radians and then substituted into the formula), λ – the wavelength of the incident beam in the diffractometer (λ = 0.154 nm), k – the Scherrer constant (k = 0.89) and d – the crystal cell parameter along the fibre axis direction (d = 1.29 nm).

TG/DTG-DSC testing

Para-aramid fibre samples underwent TG/DTG-DSC curve testing, with nitrogen gas flowing at a rate of 60–70 mL/min to create a protective atmosphere. The heating rate was set to 20°C/min.

Mechanical property testing

Referring to the American material standard ASTM D885-2010A, the para-aramid long filaments were twisted to 60 twists/meter. A constant temperature and humidity test chamber was set to the standard environment (20°C, 65% relative humidity) for humidity conditioning for 24 hours. Then, using a universal material testing machine with a clamp length of 250 mm and a stretching speed of 120 mm/min, the breaking strength and elongation at the break of the para-aramid long filament samples were tested (for each temperature point, 30 sets of degradation samples were tested).

RESULTS AND DISCUSSION

Microscopic morphological analysis

Scanning electron microscope (SEM) images of para-aramid fibre's microscopic morphology are shown in figure 1. From the SEM images, it can be observed that before reaching 350°C, the surface of para-aramid fibres is smooth and clean, with relatively high reflectivity. After treatment at 500°C, the surface of para-aramid fibres exhibits granular protrusions and a minimal number of pits. This indicates that the fibre surface undergoes oxidation to varying degrees due to the influence of high-temperature treatment. It can be seen that after heat treatment, the surface friction coefficient of para-aramid fibres increases, which can effectively enhance the binding force of the fibres, making it easier to use para-aramid fibres in the weaving of special garments such as firefighting suits and bulletproof vests. Additionally, the increase in the specific surface area of para-aramid fibres improves their dyeability to a certain extent.

Thermal property analysis

The thermal property test curves for para-aramid fibres are shown in figure 2. Observing the trends of the four DSC-TG curves in figure 2, it can be seen that the overall heating process can be divided into three stages. The first stage occurs between room temperature and 150°C, where the mass loss is primarily due to the evaporation of free water, bound water, and molecular crystalline water within the fibres. This stage is characterized by an endothermic peak, corroborating the absorption of moisture evaporation. The second stage, occurring between 200°C and 500°C, exhibits a slight decrease in fibre mass, indicating that the temperatures within this range are insufficient to cause significant degradation of the para-aramid fibre's internal molecular chains. Combining the results from table 1, which includes characteristic viscosity and dissolution characteristics of para-aramid fibre samples, it can be observed that the characteristic viscosity of para-aramid fibres remains relatively stable up to 200°C, with minor changes as the processing temperature increases. At 350°C, partial solubility is observed, resulting in a decrease in characteristic viscosity. This is mainly due to the initial reduction in characteristic viscosity resulting from the thermal oxidative degradation of

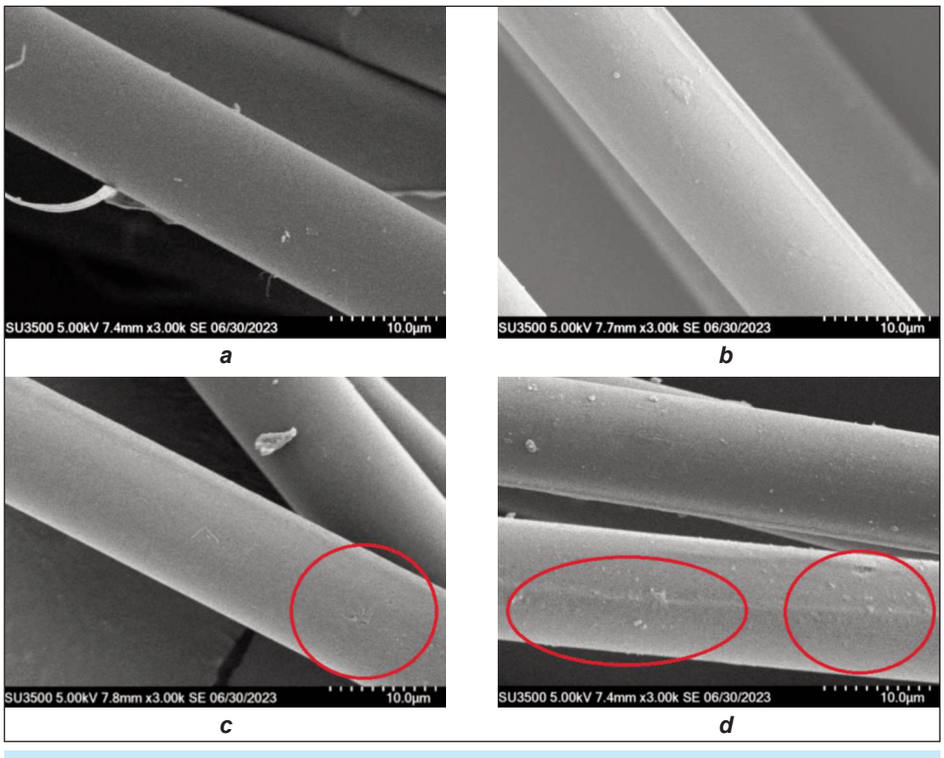

Fig. 1. Scanning electron microscope images of para-aramid fibre's microscopic morphology: *a* – 20°C; *b* – 200°C; *c* – 350°C; *d* – 500°C

molecular chain segments in para-aramid fibres. The appearance of partial solubility and insolubility at this point is attributed to the cross-linking reactions occurring in the molecular chain segments of para-aramid fibres. According to Downing and Newell [17], at temperatures below 350°C, thermal-oxidative degradation and molecular cross-linking reactions have a minimal impact on the characteristic viscosity of para-aramid fibres. However, when the temperature surpasses 350°C, para-aramid fibres exhibit varying degrees of thermal oxidative degradation and molecular cross-linking reactions. With increasing temperature, the proportion of cross-linking reactions becomes more prominent.

Referring to the DSC-TG curves for the second stage (200–500°C), it can be observed that, while para-aramid fibres undergo thermal oxidative degradation and molecular cross-linking within their internal molecular chains, the magnitude of these effects is relatively small. This indicates that a significant amount of fibre molecular chain segments remain intact and unlinked, thus preserving the fibre's properties. This will be further confirmed in subsequent sections through infrared spectroscopy and mechanical property testing. The third stage, occurring above 500°C, exhibits a substantial reduction in mass for para-aramid fibres, accompanied by a significant endothermic peak. During this stage, extensive chain fragmentation and cross-linking reactions occur within the para-aramid fibre's molecular chain segments, ultimately leading to carbonization.

Based on the DSC-TG curves, the rate of mass loss (α) for para-aramid fibre samples at any time t can be determined. By substituting this rate into the Arrhenius equation, the thermal degradation kinetic equation (equation 4) for para-aramid fibre samples can be obtained:

$$\frac{d\alpha}{dt} = A\,e^{-E/RT} f(\alpha) = A\,e^{-E/RT}(1-\alpha)^n \qquad (4)$$

In the equations below, E is the activation energy of para-aramid fibre samples, A – the frequency factor, R – the gas constant, T – the absolute temperature, and n – the reaction order.

In the DSC-TG experiments, the heating rate (experiment parameter setting) $\beta = dT/dt$ can be substituted into equation 4, simplifying it into equation 5:

$$\frac{d\alpha}{dt} = \frac{A}{\beta} e^{-E/RT} f(\alpha) = \frac{A}{\beta} e^{-E/RT}(1-\alpha)^n \qquad (5)$$

By integrating both sides of equation 5, when $n \neq 1$, equation 6 can be derived:

$$\ln\left[\frac{1-(1-\alpha)^n}{T^2(1-n)}\right] = \ln\left[\frac{AR}{\beta E}\left(1-\frac{2RT}{E}\right)\right] - \frac{E}{ER} \qquad (6)$$

When $n = 1$, formula 7 can be obtained:

$$\ln\left[\frac{-(1-\alpha)^n}{T^2}\right] = \ln\left[\frac{AR}{\beta E}\left(1-\frac{2RT}{E}\right)\right] - \frac{E}{ER} \qquad (7)$$

For typical reaction temperature ranges and activation energies, RT/E is much smaller than 1. In other words, $(1-2RT/E)$ can be approximated as 1. By selecting an appropriate reaction order n that satisfies the reaction kinetics, a linear approximation can be obtained by plotting $1/T$ on the left side. If it matches the reaction order, an approximate straight line can be drawn. The slope of this line corresponds to $-E/R$. The intercept on the vertical axis represents $\ln(AR/\beta E)$. Using this information, the activation energy E can be calculated, as shown in table 1. The calculated activation energy values for para-aramid fibre samples align with the reported range of 42.0 to 57.8 kJ/mol in the literature [25, 26]. Within this range, an n value of 2 is determined, indicating that the thermal degradation of para-aramid fibres follows second-order reaction kinetics.

Further observation of the TG curves in the four DSC-TG plots shows that the weight of the para-aramid fibres treated at high temperatures decreases at 1100°C compared to 20°C, to varying degrees. This is due to the thermal oxygen degradation and molecular crosslinking reactions exhibited by the para-aramid fibres after high-temperature treatment. With the increase in temperature, there is a transition from thermal oxygen degradation of molecular chain segments to molecular crosslinking reactions, leading to a declining trend in the orientation degree of the molecular structure, showing a disorientation trend. The non-crystalline regions are further opened up (this part is verified in the subsequent molecular structure section), exacerbating the thermal loss of fibre mass.

Molecular structure analysis

The curves related to molecular structure analysis are shown in figure 3. The infrared spectroscopy curve of para-aramid fibre samples is presented in figure 3, *a*). According to reference [27], the thermal decomposition of para-aramid fibre occurs through uninitiated decomposition, with the main molecular chain segments undergoing decomposition on the main chain. This involves the C-O bonds and C-N bonds of the amide groups, as well as C (aromatic

Table 1

TEST RESULTS FOR CHARACTERISTIC VISCOSITY, DISSOLUTION CHARACTERISTICS, AND ACTIVATION ENERGY OF PARA-ARAMID FIBRE SAMPLES

Test parameters	Temperature (°C)			
	20	200	350	500
Inherent viscosity ($dl \cdot g^{-1}$)	7.189	7.211	Slightly insoluble	Partially insoluble
Activation energy, E ($kJ \cdot mol^{-1}$)	49.42	49.13	48.94	48.55

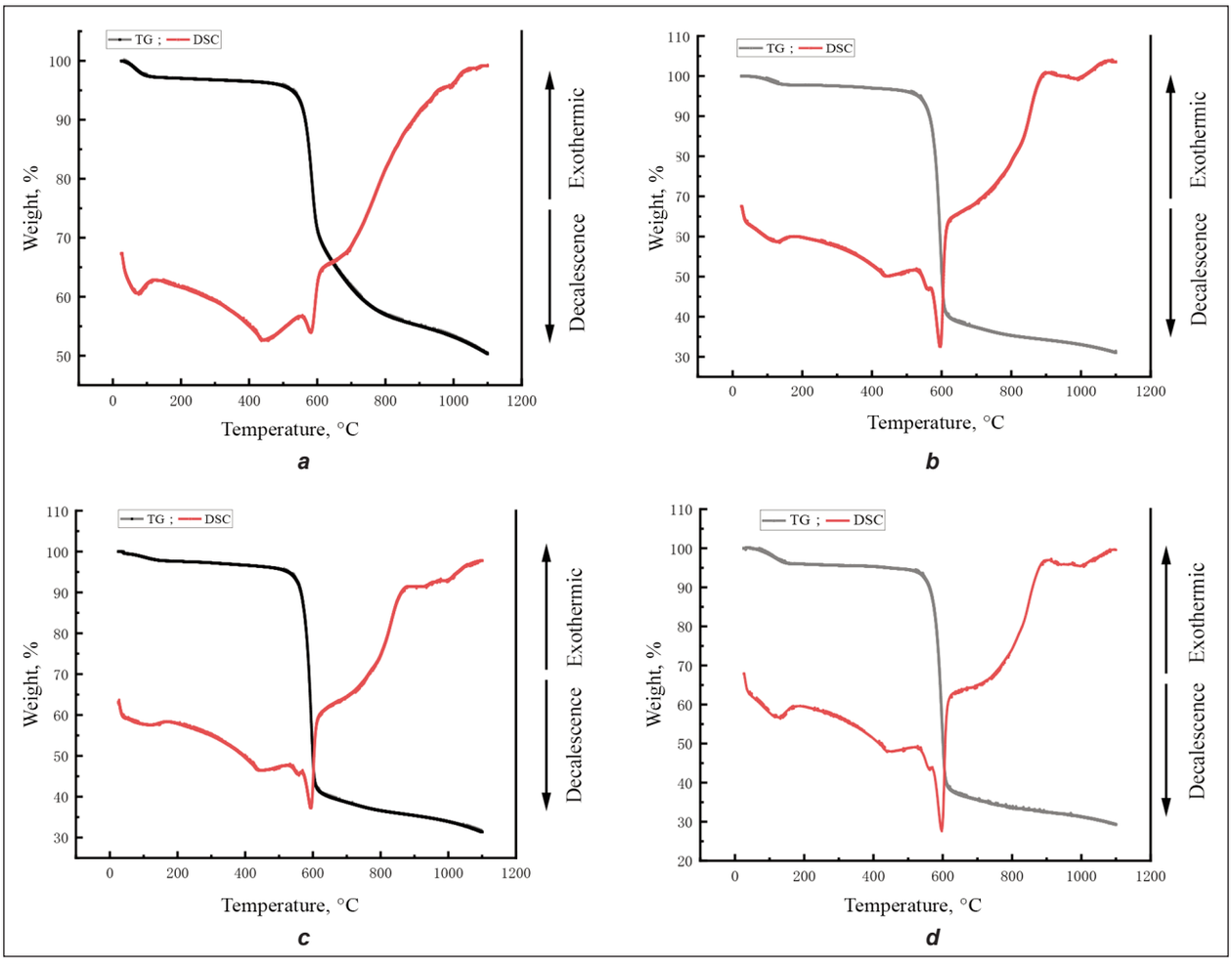

Fig. 2. Thermal properties testing curve of para-aramid fibre: *a* – 20°C; *b* – 200°C; *c* – 350°C; *d* – 500°C

ring) -C (carboxyl), C (aromatic ring) -N. At 20°C, within the range of 3325–3025 cm^{-1} corresponding to the aromatic groups, there is no significant change in absorption peaks. However, the infrared spectroscopy curves at 200°C, 350°C, and 500°C exhibit slight variations in absorption peaks, indicating a slight fragmentation of the aromatic groups due to the electronic shift of N-H and the weakening of hydrogen bonds upon temperature treatment.

The characteristic peaks, such as the amide I band at 1640 cm^{-1}, the amide II band at 1540 cm^{-1}, the amide III bands at 1260 cm^{-1}, 650 cm^{-1}, and 520 cm^{-1}, and the amide V band at 720 cm^{-1}, remain in approximately the same positions after high-temperature treatment of the para-aramid fibre, with a slightly increased intensity. This suggests that although there is some degree of fragmentation and cross-linking within the molecular chain segments of the para-aramid fibre under these conditions, the extent of these changes is relatively small. At 1050 cm^{-1}, there is an absorption peak corresponding to the fragmentation of C-N bonds in the amide groups, indicating that the molecular chain segments in the para-aramid fibre samples have undergone significant fragmentation and cross-linking, consistent with the analysis of decomposition temperatures in the DSC-TG curves mentioned earlier.

Combining the results of molecular structure parameter tests of para-aramid fibre samples in table 2, it can be seen that below 350°C, the crystallinity of para-aramid remains stable. As the temperature further increases, the crystallinity of the fibres shows an increasing trend. This is because, at a certain temperature, the amorphous regions inside the fibres undergo cleavage first, thereby reducing the proportion of amorphous regions and increasing the crystallinity of the fibres.

The orientation degree and the second-class lattice distortion rate of para-aramid fibre both exhibit a continuous decreasing trend. The decrease in orientation degree is primarily due to the unravelling of amorphous molecular chains, which inevitably results in a decrease in fibre mechanical properties, as will be verified in the subsequent mechanical performance testing. The decrease in the second-class lattice distortion rate with increasing temperature is attributed to the microcrystalline structure of the para-aramid fibre, which exhibits long-range disorder and short-range order, causing incomplete alignment and stacking of adjacent molecular chains. The apparent grain size of the 110, 200, and 002 crystal planes in para-aramid fibre increases to varying degrees with

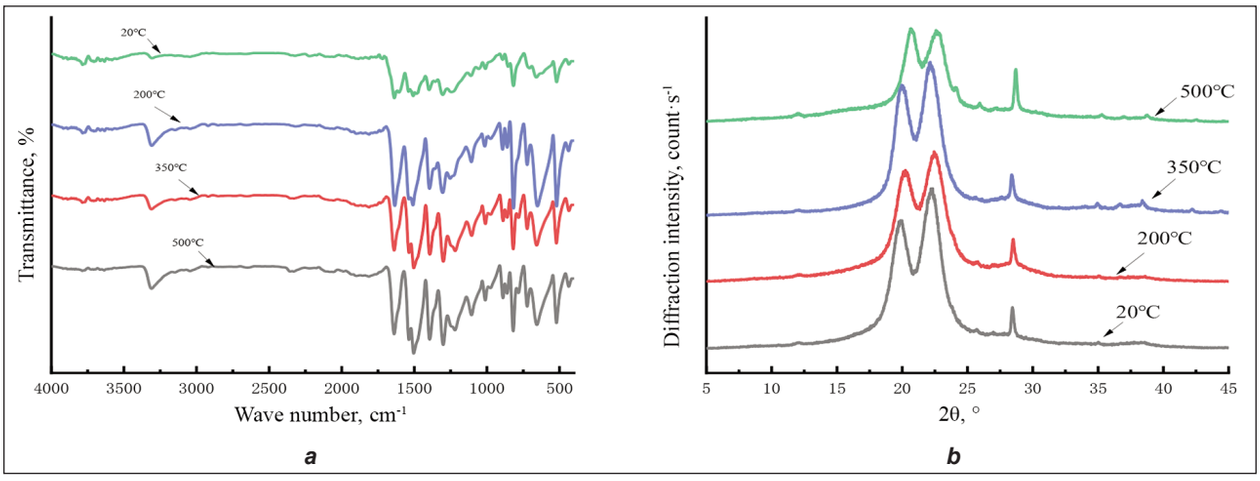

Fig. 3. Molecular structure-related test curves: *a* – infrared spectroscopy curve; *b* – X-ray diffraction curve

Table 2

CALCULATED RESULTS OF MOLECULAR STRUCTURE PARAMETERS FOR PARA-ARAMID FIBRE SAMPLES

Temperature (°C)	Crystallinity (%)	Orientation degree (%)	Second-class lattice distortion rate (%)	The apparent grain size of crystal planes		
				110 crystal plane (nm)	200 crystal plane (nm)	002 crystal plane (nm)
20	75.51	90.58	2.18	4.73	4.22	52.55
200	75.39	90.16	2.14	5.49	4.47	54.26
350	75.17	90.05	2.07	6.77	4.82	56.33
500	79.14	88.79	1.93	8.18	5.16	57.82

increasing temperature, with the increase in grain size for the 110 and 200 crystal planes being greater than that for the 002 crystal plane. This is because the arrangement of molecular chains in para-aramid fibre is distributed along the fibre axis, with some constraints on the amorphous molecular chains. The amorphous molecular chains distributed perpendicular to the fibre axis can merge laterally through conformational alignment, leading to significant growth.

The decrease in the second-class lattice distortion rate and the increase in apparent grain size of the 110, 200, and 002 crystal planes with increasing temperature indicate structural changes in para-aramid fibre to ensure the stability of the molecular structure during the process of structural decomposition, confirming the analysis of thermal properties and molecular structural changes mentioned earlier.

Mechanical performance analysis

The mechanical performance test curves are shown in figure 4. From the curves in the figure, it can be observed that the tensile strength of para-aramid fibres remains relatively stable until 200°C. However, beyond 200°C, the tensile strength of the fibres rapidly decreases, and the elongation at break increases significantly. This observation is consistent with the thermal and molecular structural analyses discussed above. Based on the previous analysis, it can be inferred that at temperatures below 200°C, the molecular structure of para-aramid fibres remains relatively stable. However, when the temperature exceeds 200°C, the molecular structure within the amorphous region of the fibres gradually undergoes cleavage and non-crystalline molecular chain disorientation, increasing the number of weak points for fibre fracture. Additionally, the crystallite size increases while the degree of orientation decreases, reducing the interfacial area of para-aramid fibres treated at high temperatures. This leads to a decreased alignment between the molecular arrangement direction and the fibre axial direction, causing a decrease in the strength of the fibres. Conversely, the elongation at break exhibits an increasing trend. From this

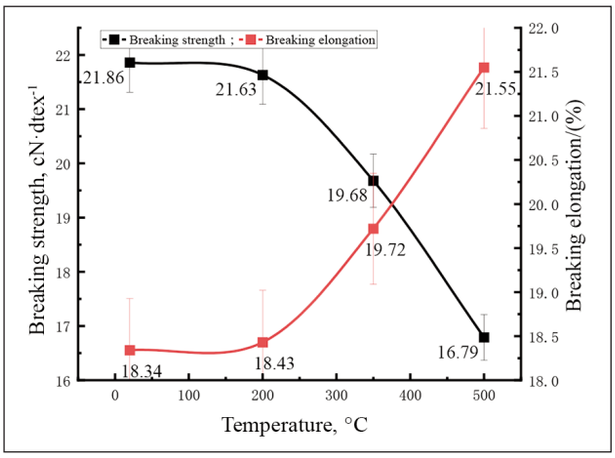

Fig. 4. Mechanical performance test curves

perspective, it can be concluded that in the design and production of para-aramid fibres, reducing the size of fibre crystallites and increasing fibre orientation can improve the mechanical properties of the fibres and reduce their degradation under high-temperature conditions.

CONCLUSION

Through the study of the thermal degradation properties and mechanisms of para-aramid fibres, it was found that after high-temperature treatment, different protruding particles and pits appear on the surface of the fibres, and the molecular structure gradually undergoes cleavage and cross-linking. This leads to varying degrees of increase in the crystallinity, intrinsic viscosity, and the apparent grain size of crystal planes in different directions of the para-aramid fibres as the temperature rises. On the other hand, the degree of orientation, the rate of the second type of lattice distortion, thermal performance, and mechanical properties show a declining trend. The thermal degradation conforms to the kinetics of a second-order reaction. The conclusions drawn from this study can provide a reference for the design and production of crystallite size and orientation of para-aramid fibres. It can also provide theoretical support for the design temperatures of firefighting suits, heat-resistant gloves, as well as vehicle and aircraft tyre cord threads, among others. It should be noted that the experiments in this study were limited to temperatures below 500°C, and an analysis of the thermal degradation mechanisms of para-aramid fibres at higher temperatures was not conducted. The study also focused on para-aramid fibres and did not investigate the high-temperature resistance of finished products made from para-aramid fibres. In the future, research will be conducted on the thermal degradation performance of fabrics made from para-aramid fibres, to reduce the thermal degradation of para-aramid fibre products and extend their service life from a fabric perspective.

ACKNOWLEDGEMENTS

This paper was financially supported by the Science and Technology Research Project of the Jiangxi Provincial Education Department (GJJ2202802; GJJ202417).

REFERENCES

[1] Rebouillat, S., Peng, J.C.M., Donnet, J.B., *Surface structure of Kevlar® fibre studied by atomic force microscopy and inverse gas chromatography*, In: Polymer, 1999, 40, 26, 7341–7350, http://doi.org/10.1016/S0032-3861(99)00040-3

[2] Morgan, R.J., Pruneda, C.O., Steele, W.J., *The relationship between the physical structure and the microscopic deformation and failure processes of poly (p-phenylene terephthalamide) fibres*, In: Journal of Polymer Science: Polymer Physics Edition, 1983, 21, 9, 1757–1783, http://doi.org/10.1002/pol.1983.180210913

[3] Kunugi, T., Watanabe, H., Hashimoto, M., *Dynamic mechanical properties of poly (p-phenyleneterephthalamide) fibre*, In: Journal of Applied Polymer Science, 1979, 24, 4, 1039–1051, http://doi.org/10.1002/app.1979.070240417

[4] Li, J., Tian, W., Yan, H., He, L., Tuo, X., *Preparation and performance of aramid nanofibre membrane for separator of lithium ion battery*, In: Journal of Applied Polymer Science, 2016, 133, 30, http://doi.org/10.1002/app.43623

[5] Cao, K., Siepermann, C.P., Yang, M., Waas, A.M., Kotov, N.A., Thouless, M.D., Arruda, E.M., *Reactive aramid nanostructures as high-performance polymeric building blocks for advanced composites*, In: Advanced Functional Materials, 2013, 23, 16, 2072–2080, http://doi.org/10.1002/adfm.201202466

[6] Park, B., Lee, W., Lee, E., Min, S.H., Kim, B.S., *Highly tunable interfacial adhesion of glass fibre by hybrid multilayers of graphene oxide and aramid nanofibre*, In: ACS Applied Materials & Interfaces, 2015, 7, 5, 3329–3334, http://doi.org/10.1021/am5082364

[7] Brown, J.R., Ennis, B.C., *Thermal analysis of Nomex and Kevlar fibres*, In: Textile Research Journal, 1977, 47, 1, 62–66, http://doi.org/10.1177/004051757704700113

[8] Brown, J.R., Power, A.J., *Thermal degradation of aramids – Part I: Pyrolysis/gas chromatography/mass spectrometry of poly(1,3-phenylene isophthalamide) and poly(1, 4-phenylene terephthalamide)*, In: Polymer Degradation and Stability, 1982, 4, 5, 379–392, http://doi.org/10.1016/0141-3910(82)90044-1

[9] Brown, J.R., Power, A.J., *Thermal degradation of aramids – Part II: Pyrolysis/gas chromatography/mass spectrometry of some model compounds of poly(1,3-phenylene isophthalamide) and poly(1,4-phenylene terephthalamide)*, In: Polymer Degradation and Stability, 1982,4, 6, 479–489, http://doi.org/10.1016/0141-3910(82)90018-0

[10] Brown, J.R., Hodgeman, D.K.C., *An e.s.r. study of the thermal degradation of Kevlar 49 aramid*, In: Polymer, 1982, 23, 3, 365–368, http://doi.org/10.1016/0032-3861(82)90336-6

[11] Khanna, Y.P., Pearce, E.M., *Aromatic polyamides. V. substituent effect on thermal properties*, In: Journal of Applied Polymer Science, 1982, 27, 6, 2053–2064, http://doi.org/10.1002/app.1982.070270618

[12] Wu, Z.Q., Zhao, Z.Q., Ye, Z.W., Qian B.J., *The Effects of Heat-Treatment on the Macro-Molecular Structure of the PPTA Fibre by GPC-[η] Method*, In: Journal of Textile Research, 1984, 5, 5, 261–266, http://doi.org/10.13475/j.fzxb.1984.05.001

[13] Hindeleh, A.M., Abdo, S.M., *Effects of annealing on the crystallinity and microparacrystallite size of Kevlar 49 fibre*, In: Polymer, 1989, 30, 2, 218–224, http://doi.org/10.1016/0032-3861(89)90108-0

[14] Zhang, Q., Liang, Y., Warner, S.B., *Partial carbonizationof aramid fibres,* In: Journal of Polymer Science Part B: Polymer Physics, 1994, 32, 13, 2207–2220, http://doi.org/10.1002/polb.1994.090321308

[15] Yue, C.Y., Sui, G.X., Looi, H.C., *Effects of heat treatment on the mechanical properties of Kevlar-29 fibre,* In: Composites science and technology, 2000, 60, 3, 421–427, http://doi.org/10.1016/S0266-3538(99)00137-2

[16] Iyer, V.R., Vijayan, K., *Effect of thermal spikes on the structural characteristics of Kevlar fibres,* In: Journal of Materials Science, 2000, 35, 22, 5731–5739, http://doi.org/10.1023/A:1004870827838

[17] Downing, J.W., Newell, J.A., *Characterization of structural changes in thermally enhanced Kevlar-29 fibre,* In: Journal of Applied Polymer Science, 2004, 91, 1, 417–424, http://doi.org/10.1002/APP.13021

[18] Wang, X.W., Hu, Z.M., Liu, Z.F., *Thermal Degradation Process of PBO Fibre,* In: Journal of East China University of Science and Technology, 2008, 34, 2, 235–241, http://doi.org/10.14135/j.cnki.1006-3080.2008.02.012

[19] Cai, R.Q., Peng, T., Wang, F.D., Ye, G.D., Xu, J.J., *Comparison of thermal decomposition behaivor of aramid fibres II and III,* In: China Synthetic Fibre Industry, 2010, 33, 4, 14–17, http://doi.org/10.3969/j.issn.1001-0041.2010.04.005

[20] Zhu, F.L., Feng, Q.Q., Xin, Q., Zhou, Y., *Thermal degradation process of polysulfone aramid fibre,* In: Thermal Science, 2014, 18, 5, 1637–1641, http://doi.org/10.2298/TSCI1405637Z

[21] Naveen, J., Jawaid, M., Zainudin, E.S., Sultan, M.T.H., Yahaya, R., Abdul Majid, M.S., *Thermal degradation and viscoelastic properties of Kevlar/ Cocos nucifera sheath reinforced epoxy hybrid composites,* In: Composite Structures, 2019, 219, 194–202, http://doi.org/10.1016/j.compstruct.2019.03.079

[22] Rao, Y., Waddon, A.J., Farris, R.J., *Structure–property relation in poly (p-phenylene terephthalamide) (PPTA) fibres*, In: Polymer, 2001, 42, 13, 5937–5946, http://doi.org/10.1016/S0032-3861(00)00905-8

[23] Ahtee, M., *An X-ray diffraction method for determination of crystallinity in wood pulp*, In: Pap Puu-Pap Tim, 1983, 65, 475–480, http://doi.org/10.1080/02773818308085176

[24] Bohn, A., Fink, H.P., Ganster, J., Pinnow, M., *X-ray texture investigations of bacterial cellulose*, In: Macromolecular Chemistry and Physics, 2000, 201, 15, 1913–1921, http://doi.org/10.1002/1521-3935(20001001)201:15<1913::AID-MACP1913>3.0.CO;2-U

[25] Auerbach, I., *Kinetics for the tensile strength degradation of nylon and kevlar yarns*, In: Journal of Applied Polymer Science, 1989, 37, 8, 2213–2227, http://doi.org/10.1002/app.1989.070370813

[26] Hall III, W.R., Knoff, W.F., *Heat aged tensile strength retention of poly (p-phenylene terephthalamide) sewing thread*, In: Journal of Engineered Fibres and Fabrics, 2008, 3, 4, 155892500800300403, http://doi.org/10.1177/155892500800300403

[27] Castro-Muñiz, A., Martínez-Alonso, A., Tascón, J.M., *Porosity development in chars from thermal decomposition of poly (p-phenylene terephthalamide)*, In: Polymer Degradation And Stability, 2009, 94, 10, 1890–1894, http://doi.org/10.1016/j.polymdegradstab.2009.06.017

Authors:

CHUNYAN ZHU[1], YANPING LIN[1], XIANGAI ZHANG[2], CHEN YANG[1,3]

[1]Jiangxi Institute of Fashion Technology, Jiangxi Centre for Modern Apparel Engineering and Technology,
No. 108, Lidu Middle Avenue, Xiangtang Economic Development Zone, 330201, Nanchang City, China
ORCID: 0000-0002-4399-7619, e-mail: tree_0206@hotmail.com

[2]Guangdong Technology College, Institute of Arts and Design,
No.3 Qifu Street Gaoyao District, 526100, Zhaoqing City, China
ORCID: 0009-0007-3773-3792, e-mail: 782131548@qq.com

[3]Hainan Normal University, Institute of Fine Arts,
No. 99 Longkun South Road, 571158, Haikou City, China

Corresponding authors:

YANPING LIN
ORCID: 0009-0005-7851-2924, e-mail: 42579825@qq.com

CHEN YANG
ORCID: 0000-0003-1593-7739, e-mail: comradeyang@qq.com